Plasma Sources Science and Technology

Comparison between a two-dimensional simulation and a global conservation model for a compact ECR plasma source

Plasma Sources Sci. Technol. 4 (1995) 22–30. Printed in the UK

Comparison between a two-dimensional simulation and a global conservation model for a compact ECR plasma source

Han-Ming Wu†, David B Graves‡ and Robert K Porteous§

Department of Chemical Engineering, University of California, Berkeley, CA 94720, USA

Received 29 September 1993, in final form 16 October 1994

Abstract. We compare results from a two-dimensional simulation of plasma transport in a compact electron cyclotron resonance (ECR) source with predictions from a spatially averaged global model based on particle and energy conservation. Model predictions include plasma density, plasma potential and electron temperature. In addition, the models predict the fraction of input power lost to various processes in the plasma. The models agree to within about 10% over the conditions examined: 0.5–10 mTorr and 850–1500 W in a model argon gas. The global model can be used to establish scaling laws, and it also provides insight into the overall plasma behaviour in terms of general conservation principles. The two-dimensional simulation is essential when spatial profile information is crucial, such as for predictions of plasma uniformity.

1. Introduction

New plasma sources are being explored and used for the manufacture of ultra-large scale integrated circuits [1]. Applications include submicrometre feature etching, film deposition and surface cleaning. Plasma process objectives include operation at low gas pressure and high plasma density to ensure collisionless ion motion through thin sheaths. If ions do not experience collisions as they are accelerated through sheaths, their motion is more anisotropic and it is possible to etch high aspect ratio features. Efficient coupling of power into electrons in the discharge allows the maintenance of a relatively high density plasma ($>10^{17}\,m^{-3}$) at relatively low neutral gas pressure (<10 mTorr). Sometimes magnetic fields are used to help confine electrons, helping to increase plasma density at a given power input. In the case of electron cyclotron resonance (ECR) discharges, the applied magnetic fields are necessary for the microwave power deposition mechanism. These characteristics enable anisotropic, relatively contamination-free etching of high aspect ratio features at acceptable rates. In addition, most new sources operate with some form of independent control of ion flux and energy to substrate surfaces. Typically, the plasma density is maintained by some inductive or wave-coupled source into electrons (e.g. ECR, RF inductive, helicon, etc.), and the substrate to be processed has applied to it an RF bias to establish a self-bias voltage. This self-bias voltage can be used to primarily adjust ion impact energy, while the plasma density controls ion flux to the surface.

In this paper, we compare results from a two-dimensional hybrid (fluid electron–particle ion) model of a magnetized ECR source in the so-called 'compact' or 'close-coupled' configuration, with predictions from a global model based on particle and energy conservation. Both modelling schemes have previously been presented, but this paper provides a direct comparison for the first time. The two-dimensional hybrid model is described in detail by Porteous *et al* [2] and Graves *et al* [3]. The global model formulation is taken from Lieberman and Gottscho [1], although we note that some of the ideas presented in this recent model have been used for the analysis of glow discharges, especially positive columns [4–7].

The global model predicts spatially averaged quantities: plasma density, plasma potential (equivalently, ion impact energy) and electron temperature. Considerable insight into the discharge behaviour can be obtained from the global model, and relatively simple cause-and-effect relationships can be established between operating conditions such as pressure and applied power and the spatially averaged plasma parameters. By taking spatial averages of the corresponding quantities predicted by the two-dimensional simulation, we are able to make a comparison between the two models.

†Present address: Institute of Mechanics, Chinese Academy of Sciences, Beijing 100080, People's Republic of China.
‡Author to whom all correspondence should be addressed.
§Present address: Research School of Physical Sciences and Engineering, Australian National University, GPO Box 4, Canberra, ACT 2601, Australia.

0963-0252/95/010022 + 09$19.50

As we demonstrate below, the agreement over the range of pressure and power considered (0.5–10 mTorr and 850–1500 W) for the model gas (based on argon) is remarkably good. We find that the two models complement each other, the global model is simple and provides a clear physical interpretation for why the plasma parameters behave as they do, whereas the two-dimensional simulation helps to validate the global model and provides detailed spatial profiles, among other things. The detail provided by the simulation will be essential for applications such as tool design and analysis, but the insight provided by the global model enhances the usefulness of the detailed simulation considerably.

2. Model description

2.1. Geometry and operating conditions

The geometry of the ECR chamber is shown in figure 1. The system is cylindrically symmetric, with the dimensions indicated in figure 1. The top surface is a dielectric, through which the microwaves enter the chamber. All other surfaces are assumed to be conducting and grounded. Two sets of coils establish the diverging magnetic field (lines of force shown schematically in figure 1), with the resonant zone near the centre of the device. In this configuration, the resonant zone is fairly close to the substrate, typically within 10 cm. The main advantage of having the resonant zone close to the substrate is that plasma density is higher at the substrate surface, increasing processing rates. The neutral gas pressure and temperature are assumed to be spatially uniform. Neutral gas pressure is varied from 0.5 to 10 mTorr in the present study and the neutral temperature is assumed to be 0.06 eV [8]. We have used a model argon gas, with characteristics described below, as the neutral gas. This model for argon was used previously [2, 3]. Power into electrons is assumed to be 850 W for most of the results presented here. One case was run at 1500 W to examine the power dependence of the plasma parameters.

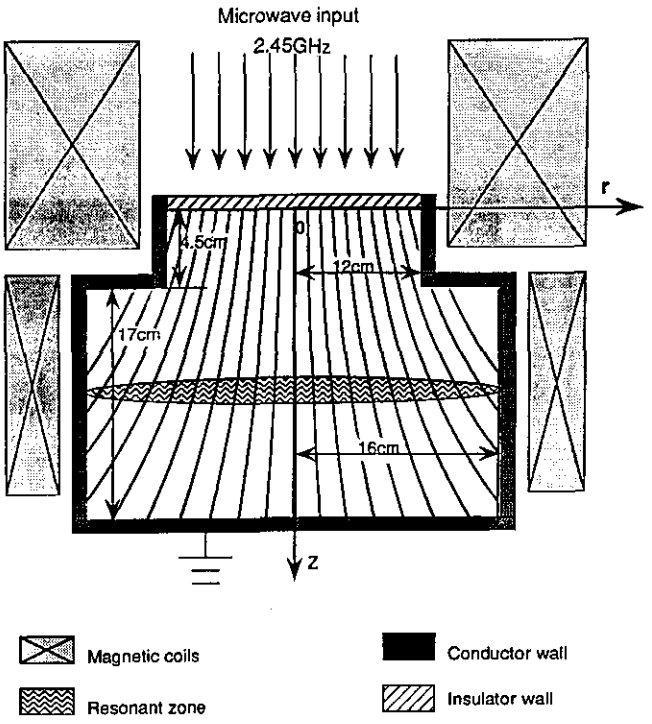

Figure 1. Schematic diagram of ECR device modelled.

2.2. Two-dimensional hybrid model

The two-dimensional hybrid model has been described in greater detail elsewhere so we provide only a summary here [2, 3]. Ions are treated as particles and electrons are treated as a Maxwellian fluid with an electron temperature T_e. Electrons are assumed to be strongly magnetized and therefore cannot cross magnetic field lines. The ionization rate spatial profile determines the rate of creation of particle ions that stream to walls under the influence of the electrostatic and magnetic fields. Ion collisions with neutrals (charge exchange and elastic) are handled with Monte Carlo techniques. Averaging over many ion trajectories yields a stable and smooth ion density spatial profile in addition to ion flux to walls.

The electron fluid model consists of electron continuity, an electron energy balance and Poisson's equation. Electron temperature is determined from the electron energy balance, a key element of which is the assumed spatial profile of the incident microwave power. Note that the microwave power profile will affect the details of the spatial profile of the electron temperature, but that the mean electron temperature will be determined from the need to balance ion creation and loss [2, 3]. We parameterize the power deposition spatial profile, with power peaking at the axial locations where the magnetic field is near the Doppler-shifted resonant value, ~950 Gauss [9]. However, the precise axial location of the resonance zone has relatively little effect on the spatial profiles because electrons move easily in the axial direction. The radial power profile is taken to peak on-axis, and as we have demonstrated elsewhere [3], this

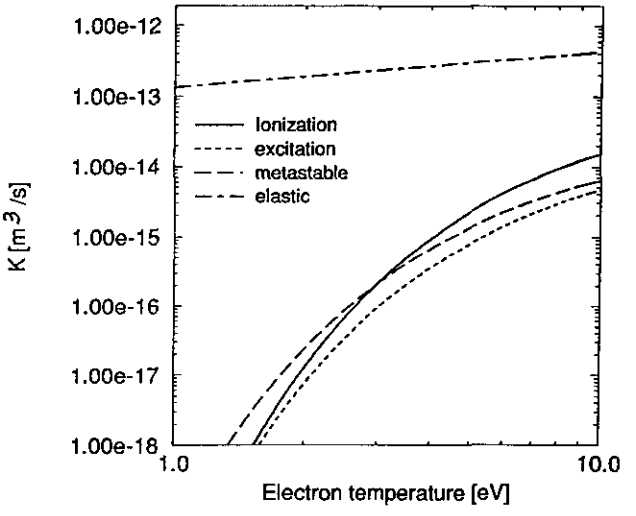

Figure 2. Rate coefficients for electron–neutral collisions as a function of electron temperature.

tends to produce a plasma density profile that peaks in the centre of the device. Although the radial power profile strongly affects details of plasma uniformity, the mean plasma density depends primarily on total power deposited. Since the purpose of this paper is to compare with a global model that is intrinsically spatially averaged, we did not attempt to adjust the power profile.

The electron energy balance includes electron–neutral collision rates. In our model argon gas, we have used the same rate expressions employed in previous papers [2, 3], with a single step ionization from ground state argon, one process representing electronic excitation to a resonant state, one process for excitation to a metastable state, and elastic collisions. Metastable atoms are not followed after they are created by electron impact. All charged–charged collisions have been neglected. As noted above, we have assumed a Maxwellian electron energy distribution function (EEDF), and have used rate coefficients based on electron temperature. We are aware, of course, that this is usually only approximately correct, although recent Thomson scattering measurements of Bowden *et al* [10] suggest that it is not a bad approximation under most conditions relevant to ECR device operation. Lieberman and Gottscho [1] make the same assumption in their global model. For the purposes of the present models, which do not purport to be quantitative, this assumption is appropriate. Of course, to make a proper comparison, the same collisional processes are used in both the two-dimensional simulation and the global model.

Electron density and plasma potential are determined from the ion density profile, electron continuity and Poisson's equation. Sheaths are not resolved numerically, but the magnitude of the sheath potential is determined by the need to balance electron and ion flow to insulated surfaces, and to ensure that electron creation and loss rates along a magnetic field line are equal. The solution strategy is iterative, and convergence is achieved when the plasma density in the centre of the discharge stops changing to within several per cent.

Typical profiles obtained from the simulation are shown in figures 3–5. Figure 3 is a plot of plasma

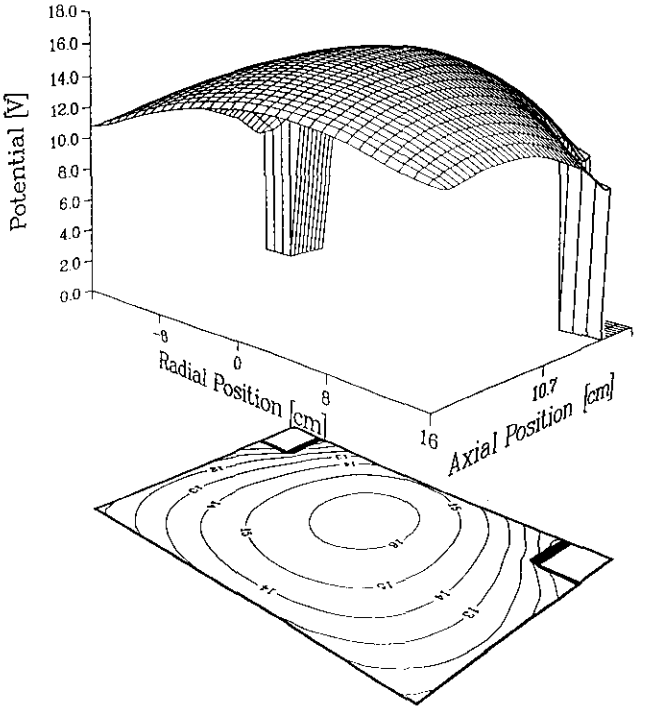

Figure 4. Plasma potential spatial profile for argon discharge at 5 mTorr and 850 W from hybrid simulation.

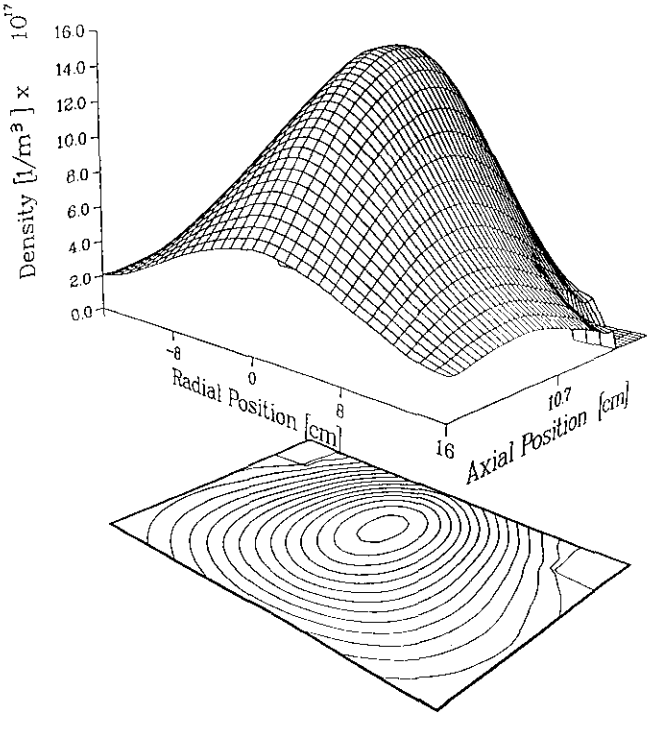

Figure 3. Plasma density spatial profile for argon discharge at 5 mTorr and 850 W from hybrid simulation.

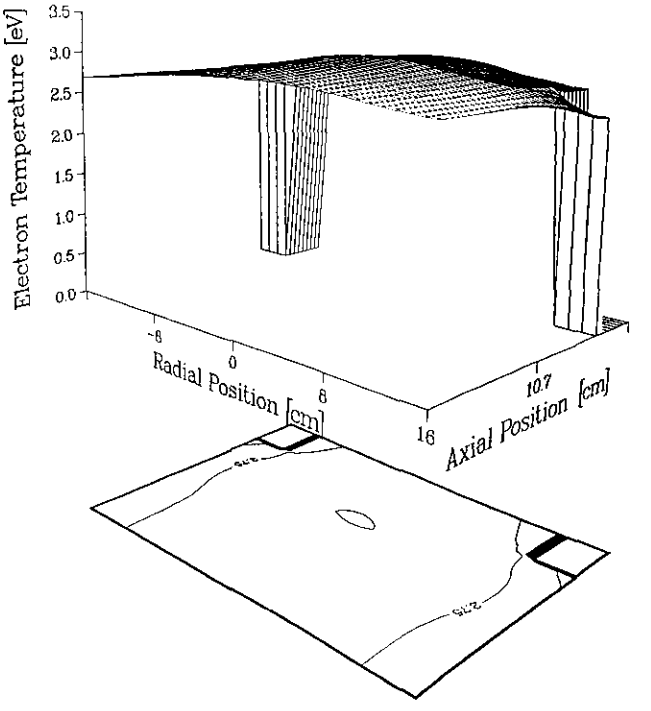

Figure 5. Electron temperature spatial profile for argon discharge at 5 mTorr and 850 W, from hybrid simulation.

density, showing the peak in density near the centre of the device at about $1.5 \times 10^{18}\,\mathrm{cm}^{-3}$, falling to about one tenth to one third that value along the walls. As noted previously, the spatial uniformity is primarily a function of the power deposition profile, but for the purposes of the comparison to the spatially averaged global model, the spatial profile is less important. Figure 4 is plasma potential in the body of the plasma. Recall sheaths are treated analytically, so the plasma potential drop in sheaths is not shown. The dielectric surface (cf. figure 1) will charge to several volts (both positive and negative values have been observed) to equate the local fluxes of electrons and ions. The remaining walls are at ground potential. Figure 5 is a plot of the predicted electron temperature profile. This quantity is nearly uniform across the volume of the device, reflecting the high electron thermal conductivity along field lines.

2.3. Global model

The basic structure of the global model can be summarized as follows [1].

(1) The positive ion continuity equation equates the global rate of creation and loss of ions. Both rates are functions of electron temperature. They are also both proportional to plasma density when charged species creation is from electron-impact ionization of ground state atoms, and loss is by ambipolar diffusion to walls. Hence, the balance between plasma creation and loss is independent of plasma density. Therefore, this equation determines electron temperature T_e as a function of the product of neutral number density N_N and discharge effective characteristic length d_{eff}.

(2) The electron continuity equation and the assumption of ambipolar plasma flow to walls determines the mean plasma potential ϕ_p as a function of electron temperature.

(3) The power balance, equating power input to the plasma to the power lost through collisions and walls loss determines plasma density N_p. In this model $N_p = N_e = N_+$.

2.3.1. Ion continuity and electron temperature. Ions (and electrons) are created by electron-impact ionization of ground state argon atoms with the following rate expression: $R_{ion} = K_{ion} N_N N_e$, where K_{ion} ($\mathrm{m}^3\,\mathrm{s}^{-1}$) is the ionization rate coefficient and $N_N(\mathrm{m}^{-3})$ neutral gas density and $N_e(\mathrm{m}^{-3})$ is electron density. The ionization rate coefficient is expressed as a function of electron temperature

$$K_{ion}(T_e) = \sigma_{ion} v_e \exp[-E_i/kT_e] \qquad (1)$$

where σ_{ion} is a constant, $v_e = (8kT_e/\pi m)^{1/2}$ is the mean electron thermal speed and E_i is the effective activation energy for ionization. All other rate coefficients for electron–neutral collisions have a similar form and the values used for each process are listed in table 1. Ions are lost from the discharge after being accelerated to the Bohm velocity $v_B = (kT_e/M)^{1/2}$ at the sheath edge,

Table 1. Constants used in rate coefficients for electron-neutral collisions: $K_j(T_e) = \sigma_j v_e(T_e) \exp[-E_j/kT_e]$.

Process i	$\sigma_j(10^{-20}\,\mathrm{m}^2)$	E_j(eV)
Ionization	3.0	15.75
Excitation to resonant levels	1.0	12.0
Excitation to metastable levels	0.9	14.1
Elastic	20.0	0.0

where M is ion mass. Equating volume ion creation and wall loss for a cylindrical source with radius R and length L,

$$K_{ion} N_N N_p \pi R^2 L = N_p v_B (2\pi R^2 h_L + 2\pi R L h_R). \qquad (2)$$

In equation (2), N_p is the peak or centre plasma density, assumed to be reasonably uniform over the volume of the plasma. Hence, on the left-hand side of (2) N_p and the total source volume are used. However, ions are lost at the plasma-sheath edge, and it is known that plasma density drops to a lower value at the sheath edge. The ratio of edge to centre line plasma density is defined for each direction, axial ($h_L = N_{sL}/N_p$) and radial ($h_R = N_{sR}/N_p$). In order to account for the way these ratios change with neutral gas density and therefore the degree of ion-neutral collisionality, Lieberman and Gottscho [1] have adopted the following estimates:

$$h_L = N_{sL}/N_p \sim 0.86(3 + L/2\lambda_i)^{-1/2} \qquad (3)$$

$$h_R = N_{sR}/N_p \sim 0.80(4 + R/\lambda_i)^{-1/2} \qquad (4)$$

where $\lambda_i = (N_N \sigma_{in})^{-1}$ is the mean free path for ion–neutral collisions. In equation (2), the bracketed term on the right-hand side can be viewed as an effective area,

$$A_{eff} = 2\pi R(Rh_L + Lh_R) \qquad (5)$$

Then, an effective length can be defined as the ratio of the source volume to effective area,

$$d_{eff} = RL/(Rh_L + Lh_R). \qquad (6)$$

Equation (2) can be written in the following form:

$$K_{ion}(T_e)/v_B(T_e) = (N_N d_{eff})^{-1}. \qquad (7a)$$

Equation (7a) can be solved directly for electron temperature kT_e:

$$kT_e = E_i/[\ln(4\sigma_{ion} N_N d_{eff}) + 4.7]. \qquad (7b)$$

If N_N and d_{eff} are known, equation (7b) can be solved. For example, for our plasma source, $R = 0.16\,\mathrm{m}$ and $L = 0.215\,\mathrm{m}$. For a neutral gas pressure $p_n = 5$ mTorr and temperature $T_n = 0.06\,\mathrm{eV}$, the neutral density is $N_N = 6.9 \times 10^{19}\,\mathrm{m}^{-3}$. The mean free path for Ar^+–Ar collisions is approximately $\lambda_i = 1/(N_N \sigma_{in}) = 0.016\,\mathrm{m}$. The Bohm velocity $v_B = 1546(kT_e)^{1/2}\ \mathrm{m\,s}^{-1}$, $h_L = 0.27$, $h_R = 0$ (ignoring radial losses because of the strong, mainly axial, magnetic field) and $d_{eff} = 0.39\,\mathrm{m}$.

For these conditions, the model predicts that electron temperature $T_e = 2.5\,eV$.

All inelastic rate coefficients, including ionization K_{ion}, electronic excitation to a resonant state K_{ex}, a metastable state K_{me}, and elastic scattering K_{el} are plotted in figure 2 as a function of electron temperature T_e.

2.3.2. Electron continuity, plasma potential and ion bombarding energy. Since electrons and ions are created at the same rate in the plasma, the loss rate of electrons and ions to walls must be equal. Along insulating surfaces, point-wise equality of electron and ion flux is exactly satisfied, and for conducting surfaces it will be very close to being satisfied. Since ions are accelerated to the Bohm velocity at the sheath edge, the magnitude of the sheath potential does not affect their flux to walls. However, electron flux to walls can be estimated to be

$$\Gamma_e = 1/4\, N_{es} v_e \exp[(\phi_w - \phi_p)/kT_e] \qquad (8)$$

where N_{es} is electron density at the plasma-sheath edge, v_e is the electron thermal speed (defined previously), ϕ_w is wall potential and ϕ_p is the plasma potential at the sheath edge. For grounded and conducting surfaces $\phi_w = 0$ and for insulating surfaces it adjusts to satisfy equality of electron and ion flux. Equation (8) is based on the assumption that electrons recombine with unity efficiency at walls and that they are in equilibrium with the sheath potential. Equating electron and ion loss to walls, we obtain the well known expression for floating potential:

$$V_s = -(\phi_w - \phi_p) = 0.5\, kT_e \ln(M/2\pi m_e). \qquad (9)$$

Since ions are accelerated to the Bohm velocity at the sheath edge (kinetic energy per ion $kT_e/2$), the ion energy impacting surfaces ε_i is given by

$$\varepsilon_i = kT_e/2 + V_s \qquad (10)$$

where M and m are ion mass and electron mass, respectively. For argon, $V_s = 4.7\,kT_e$ and $\varepsilon_i = 5.2\,kT_e$. Equations (9) and (10), when combined with the previously determined electron temperature, allow an estimate of the plasma potential (assumed to be equal to ε_i here). The plasma potential would rise above the floating potential if a significant RF bias were applied to a surface contacting the plasma, but we neglect that here.

It may seem at first that all electrons with energies greater than the sheath potential would quickly leave the discharge in their first sheath collision but this does not occur. Recall that nearly isotropic electrons have velocity components in all three velocity dimensions, and the component of electron energy (or velocity) in any one direction is less than its total energy. It can be shown that for an electron with total energy K, isotropically distributed in velocity space, the probability that a collision between the electron and the sheath results in electron escape through the sheath is $1 - [eV_s/K]^{1/2}$ if $K > eV_s$. For example, for a 30 eV electron and a 14 V sheath potential, the escape probability per electron–sheath collision is ~ 0.32.

2.3.3. Power balance and plasma density. The power absorbed by the plasma electrons from the external power source is lost in a variety of ways. These include electron–neutral collisions, both inelastic and elastic, ion–neutral collisions, and the loss of electron and ion kinetic energy when these species recombine at walls. Although all power is deposited into electrons, ions gain energy indirectly from electrons. The ambipolar electric field in the body of the plasma is maintained by electron thermal energy. By diffusing against this field, electrons lose the energy that is transferred to ions in the form of directed energy. The electron–neutral collisional losses are equal to the rates of the collisions times the energy lost per collision described below.

For a discharge in a gas like argon, in which a single ionic species and one ionization channel is assumed to dominate, it is useful to define the collisional energy lost per electron–ion pair created or ε_c. This quantity is simply the sum of the terms for each of the collisional loss processes divided by the ionization rate

$$\varepsilon_c = \varepsilon_{ion} + [K_{ex}\varepsilon_{ex} + K_{me}\varepsilon_{me} + K_{el}\varepsilon_{el}]/K_{ion} \qquad (11)$$

where $\varepsilon_{ion} = 15.75\,eV$, $\varepsilon_{ex} = 14.1\,eV$, $\varepsilon_{me} = 12\,eV$ and $\varepsilon_{el} = 3\,mkT_e/M$ are the energies lost per electron as a result of ionization, electronic excitation, metastable creation and elastic collisions, respectively. We note again that the model for electron–argon collisions is meant to be representative, not quantitative. The quantity ε_c can be seen to be a function only of T_e. ε_c is plotted in figure 6 as a function of electron temperature.

In addition to collisional energy loss, the electrons and ions carry their kinetic energy to the walls. It can be shown that the mean kinetic energy lost per electron recombining at the wall is $\varepsilon_e = 2kT_e$ [6]. The mean kinetic energy lost per ion consists of the kinetic energy of ions at the plasma-sheath edge plus the sheath potential. We ignore ion–neutral collisions in the present model and neglect the relatively small ion random thermal kinetic energy. As noted above, the kinetic

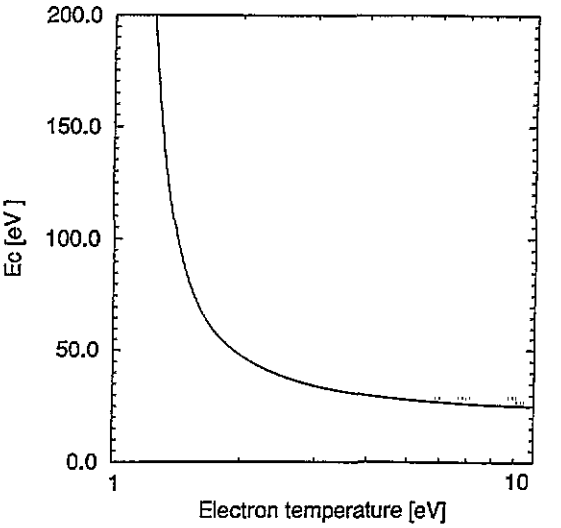

Figure 6. Parameter ε_c as a function of electron temperature: energy loss due to electron–neutral collisions per ion–electron pair created.

energy per ion flowing out of the plasma is about $5.2kT_e$ for Ar^+.

The total energy lost per electron–ion pair created in the system, ε_L, can be expressed as follows,

$$\varepsilon_L = \varepsilon_c + 5.2kT_e + 2kT_e = \varepsilon_c + 7.2kT_e \qquad (12)$$

Since ε_L is the total energy lost per electron–ion pair created, and the rate of creation of electrons and ions must equal their loss rate ($N_P v_B A_{eff}$), the overall global energy balance for the plasma can be written in terms of ε_L as

$$P_{abs} = N_P v_B A_{eff} \varepsilon_L \qquad (13)$$

where P_{abs} is power absorbed in the plasma, and the other terms have been defined previously. Equation (13) can be solved for plasma density N_P since v_B and ε_L are functions only of electron temperature, and A_{eff} can be estimated given the neutral density and device dimensions. We note that the quantity ε_L^{-1} represents the ionization efficiency of the source: ions created per Watt delivered to the plasma. This quantity has a maximum (ε_L has a minimum) at approximately 2 mTorr, corresponding to an electron temperature of ~3 eV. However, of greater interest in many processing applications is ion current to surfaces, and this quantity will be related not only to the ion production efficiency but also to ion confinement.

This completes the global model: equation (7*b*) is used to estimate T_e, equation (9) determines the plasma potential and therefore ion impacting energy and equation (13) determines plasma density.

3. Results and discussion

We now compare predictions from the global model with the simulation. Input power is set at 850 W, and we varied neutral gas pressure (assuming a neutral temperature of 0.05 eV). Figures 7–9 demonstrate the model and simulation predictions of electron temperature, ion impact energy, and plasma density, respectively. Results are plotted from 0.5 to 10 mTorr.

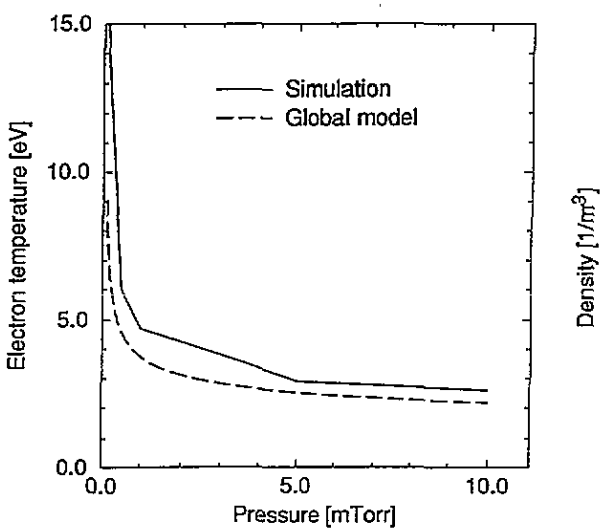

Figure 7. Comparison between global model and simulation predictions of electron temperature dependence on neutral gas pressure (850 W).

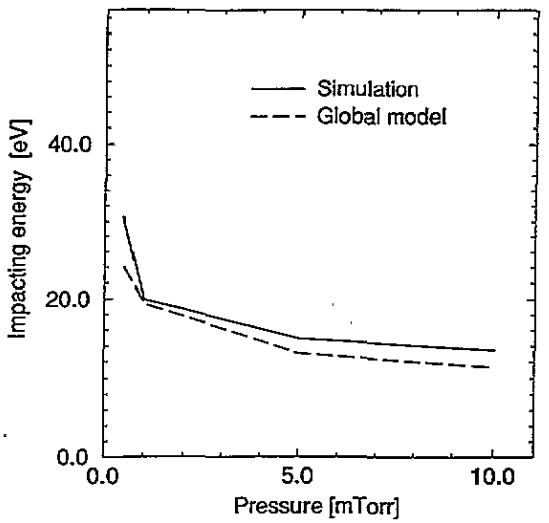

Figure 8. Comparison between global model and simulation predictions of ion impact energy dependence on neutral gas pressure (850 W).

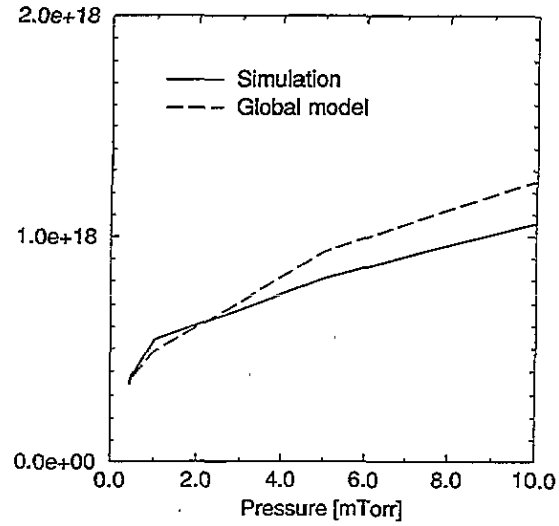

Figure 9. Comparison between global model and simulation predictions of plasma density dependence on neutral gas pressure (850 W).

Figure 7 shows that electron temperature is relatively insensitive to neutral gas pressure above about 5 mTorr, but rises rapidly as pressure is lowered below about 1 mTorr. Note that the model predicts that the relevant quantity is the product of neutral gas number density and effective discharge length, so the plots shown here will change if the device size changes. The agreement between the model and simulation is remarkably good, indicating that the global model has captured the dominant effect in setting electron temperature. Recall that the electron temperature depends on equating the rates of creation and loss of ions, both of which are functions of T_e. We emphasize a point commonly misunderstood: at steady state, *electron temperature is not directly determined by the electron energy balance, but*

rather by the ion continuity equation. In the 2 D model we use the electron energy balance equation to compute the electron temperature profile. However, it is really the ion continuity equation that determines the mean value of the electron temperature. Although we do not show it here, electron temperature in the simulation can be shown to be nearly independent of applied power [2], in agreement with the global model. The rapid rise in electron temperature at very low pressure can be explained by the fact that the ionization rate coefficient dependence on electron temperature (that is, $\partial K_{ion}/\partial T_e$) decreases markedly at relatively high T_e (cf. figure 2). As gas density decreases, the ionization rate coefficient must increase to balance ion creation and loss rates. This requires a rise in T_e, but as gas pressure is lowered sufficiently electron temperature must increase more rapidly in order to balance the drop in gas density. At some point the discharge will extinguish as T_e cannot rise enough to balance the decrease in gas density. This is equivalent to saying that no solution can be obtained to equation (*7b*) (the denominator of the right-hand side approaches zero) if the product $N_N d_{eff}$ becomes sufficiently small.

Ion wall impact energy is plotted as a function of neutral pressure in figure 8. As can be seen in equation (10), this quantity is proportional to T_e and therefore shows the same trends with pressure. Again, the agreement between the simulation and global model is quite good. Since ion impact energy is proportional to electron temperature, it also is predicted to be independent of applied power. As in the case of electron temperature, the simulation results show the same weak dependence of ion impact energy with applied power as predicted by the global model. We showed previously that the simulation predictions of the relationship between electron temperature and plasma potential, and their dependence on pressure and power, have been observed experimentally [2].

Figure 9 is a plot of plasma density as a function of gas pressure, and once again the agreement between the model and simulation is striking. At low pressure, plasma density rises relatively rapidly with pressure, then more slowly as pressure increases above about 1 mTorr. The change in slope in the plasma density plot at about 1 mTorr is correlated with the rapid rise in T_e and ion impact energy at the same point. As we discuss in more detail below, the reason for this drop in plasma density at low pressure is that the ionization efficiency of the source drops: an increasing fraction of the input power goes into maintaining the plasma potential and driving ions to walls, and a smaller fraction goes into electron-impact ionization. Equation (13) indicates that plasma density will drop if ε_L increases, and it increases rapidly at electron temperatures above about 4 eV in the model for argon collisional processes that we have used here. Figure 6 shows that the energy lost in electron–neutral collisions per ion–electron pair created *decreases* as T_e increases, but the second term in equation (12), related to the wall losses of electrons and ions, is proportional to T_e. At sufficiently high T_e, it is this latter term that dominates, accounting for the drop in ionization efficiency at low gas pressure.

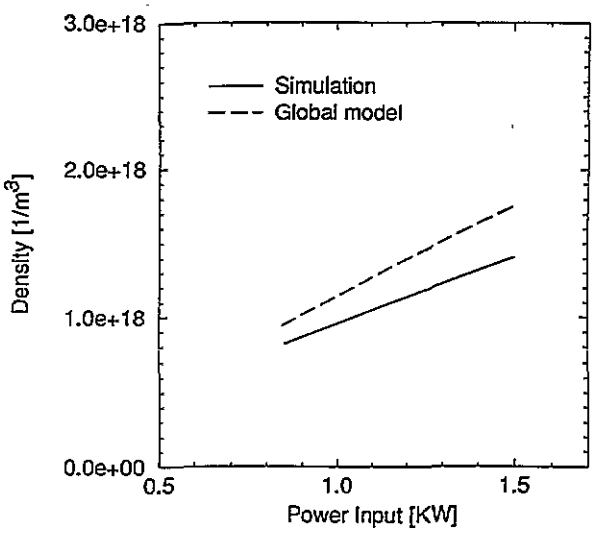

Figure 10. Comparison between global model and simulation predictions of plasma density dependence on applied power (5 mTorr).

Figure 10 plots plasma density as a function of applied power at 5 mTorr. Although the quantitative agreement is less impressive than in the previous comparisons, we see that both models predict increases in plasma density with power. The global model (equation (13)) predicts the dependence to be exactly linear, but the simulation shows a slightly sublinear dependence. However, we note that one can obtain slightly different slopes from the simulation predictions depending on how the spatial average is taken. For the purposes of the comparison, the predicted slope is essentially in agreement. In addition, the global model assumes that the radial plasma losses can be neglected ($h_R = 0$) and this is clearly an approximation since some ions and electrons are lost to the radial walls. It is really not possible to exactly capture the 2D nature of the plasma losses to bounding walls in a 0D approximation, so it is to be expected that this is a source of inaccuracy in the global model.

Finally, figures 11 and 12 are plots of the various power loss processes predicted by the global model and simulation, respectively, as a function of gas pressure at 850 W applied power. It is instructive to consider the degree to which the power balance closes, that is, whether the input power is exactly matched by the various power loss processes. The global model power balance closes exactly of course, and the 2D simulation power balance closes to less than 10% under all conditions shown. That is, the power losses are within at least 10% or less of the input power of 850 W for the simulation. Discrepancies are greatest at the lower pressure, and can be attributed mainly to the sensitivity of the global model to the value of d_{eff} on electron temperature in this regime. Figures 11 and 12 again demonstrate the relatively good agreement between the global model and the simulation. At low pressure, the main power loss is from ion wall losses, because of the rise in electron

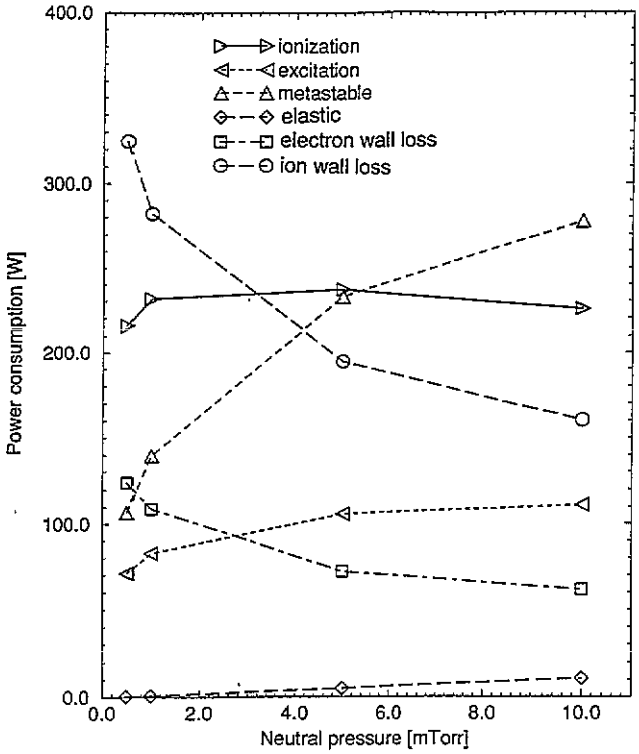

Figure 11. Power loss channels as a function of pressure (850 W) predicted from the global model.

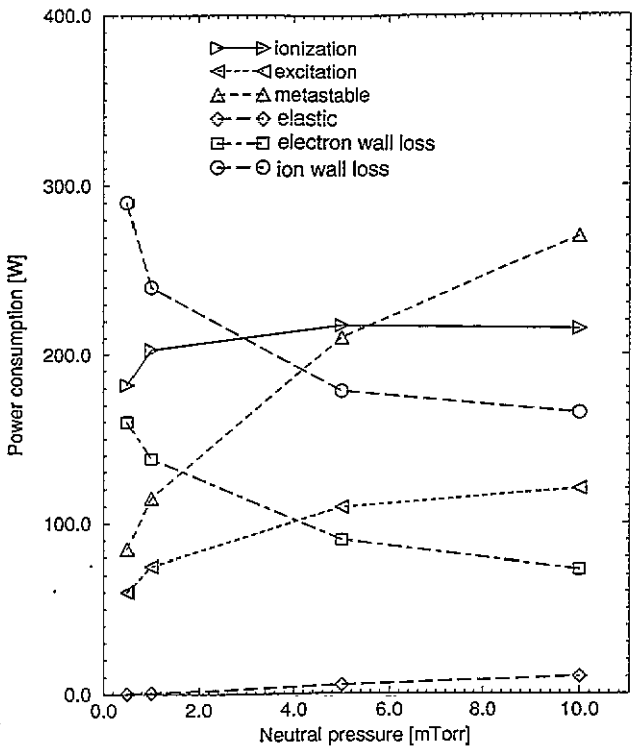

Figure 12. Power loss channels as a function of pressure predicted from the simulation. Note the relatively good agreement with figure 11. Disagreement is greatest at lower pressures, where simulation power losses are about 8% less than input power of 850 W.

temperature and plasma potential at low pressure, as discussed previously. At 10 mTorr, the largest single power loss is from metastable excitation. We caution that the specific power loss mechanisms predicted by the current model for argon are not necessarily quantitative, as we are not attempting here to make quantitative predictions concerning argon discharges. For example, we ignore ionization from metastable atoms. It suffices, for the purposes of the present paper, that the collisional rate expressions are the same in the global model and simulation so as to make a proper comparison. We note that previous efforts to compare simulation predictions to experiment demonstrate the reasonable accuracy of the model [2].

4. Conclusions

A comparison was made between a 2D hybrid simulation of an argon discharge in a 'compact' or 'close-coupled' ECR device with a global model based on particle and power balances. The global model predictions of the dependence of electron temperature, plasma potential and plasma density on gas pressure and applied power were shown to be in good agreement with the predictions of the more complete and complex simulation. The simplicity of the global model allows simple physical interpretations of simulation predictions. It should be noted that the global model and the hybrid 2D model share a number of assumptions (e.g. the Maxwellian electron fluid and the manner in which microwave power absorption is handled). Some measure of agreement between the models is to be expected, therefore.

The global model shows that electron temperature is set by the need to balance ion creation and loss and is independent of applied power. Electron temperature increases slowly as pressure is reduced until about 1 mTorr, at which point it rises rapidly. The rapid rise in electron temperature at low pressure is due to the nature of the ionization rate coefficient dependence on electron temperature: more sensitive at lower temperature (below about 3–4 eV in the current model), increasingly less sensitive at higher temperature. In order to balance ion creation and loss, temperature must rise rapidly at low gas pressure. Plasma potential is predicted to be proportional to electron temperature in order to balance electron creation and loss. It is convenient to think of plasma potential as adjusting itself so that electrons are lost to walls at the proper rate. Hotter electrons require a higher potential barrier, colder electrons require a lower barrier. Since ions are accelerated to the plasma–sheath boundary by the relatively small bulk potential drop ($\sim kT_e/2$), sheath potential does not directly affect the ion loss rate, only electron loss. Electrons maintain the plasma potential by their thermal energy, and the plasma sheath potential confines electrons to constrain their loss to be equal to the ion loss rate. The close coupling between the electron continuity equation and Poisson's equation reflects this tight physical coupling between electron density and plasma potential.

The power balance determines plasma density: density is proportional to input power and rises relatively quickly with pressure at low pressure, less rapidly at

higher pressure, over a pressure ranging from 0.5–10 mTorr. The relatively rapid drop in plasma density as pressure is lowered below about 1 mTorr in the device modelled is related to the rise in electron temperature at the same pressure. Since plasma potential is proportional to electron temperature, plasma potential and therefore power lost to ions impacting walls, increases rapidly below about 1 mTorr. As a result, the ionization efficiency decreases and the plasma density falls accordingly.

The value of even approximate global models in the interpretation of multi-dimensional simulations should be apparent. It is often difficult to extract from detailed simulations the simple, but key physical ideas concerning cause-and-effect relationships. Many trends observed experimentally can be interpreted with the aid of simple global models. Detailed simulations are essential when spatial information is needed, for example in the design and analysis of specific plasma processing tools.

Acknowledgments

The authors gratefully acknowledge R Stewart for helpful discussions on the global model description and M D Kilgore and M A Lieberman for reading and comments on the manuscript. The work was supported in part by NSF grant CTS 8957179.

References

[1] Lieberman M A and Gottscho R A 1994 in *Physics of Thin Films*, ed. by M Francombe and J Vossen Academic Press 1
[2] Porteous R K, Wu H-M and Graves D B 1993 *Plasma Sources Sci. Technol.* **3** 25
[3] Graves D B, Wu H and Porteous R K 1993 *Jpn. J. Appl. Phys.* **32** 2999
[4] Langmuir I and Tonks L 1929 *Phys. Rev.* **34** 876
[5] von Engel A 1965 *Ionized Gases* 2nd edition, Oxford University Press, London
[6] Golant V E, Zhilinsky A P, Sakharov I E and Brown S C 1980 *Fundamentals of Plasma Physics* (New York: Wiley)
[7] Ferreira C M and Ricard A 1983 *J. Appl. Phys.* **54** 2261
[8] Nakano T, Sadeghi N and Gottscho R A 1991 *Appl. Phys. Lett.* **58**
[9] Stevens J E, Huang Y C, Jarecki R L and Cecchi J L 1992 *J. Vac. Sci. Tech.* A **10** 1270
[10] Bowden M D, Okamoto T, Kimura F, Muta H, Uchino K, Muraoka K, Sakoda T, Maeda M, Manable Y, Kitagawa M and Kimura T 1993 *J. Appl. Phys.* **73** 2732